Research Paper

GEOSPHERE

GEOSPHERE, v. 14, no. 6

https://doi.org/10.1130/GES01697.1

10 figures

CORRESPONDENCE: fernando.martinez@ucn.cl

CITATION: Fuentes, G., Martínez, F., Bascuñan, S., Arriagada, C., and Muñoz, R., 2018, Tectonic architecture of the Tarapacá Basin in the northern Central Andes: New constraints from field and 2D seismic data: Geosphere, v. 14, no. 6, p. 2430–2446, https://doi.org/10.1130/GES01697.1.

Science Editor: Raymond M. Russo

Received 24 March 2018
Revision received 10 July 2018
Accepted 27 August 2018
Published online 12 October 2018

Tectonic architecture of the Tarapacá Basin in the northern Central Andes: New constraints from field and 2D seismic data

Guillermo Fuentes[1,2], Fernando Martínez[3], Sebastián Bascuñan[1], César Arriagada[4], and Rodrigo Muñoz[5]

[1]Departamento de Geología, Facultad de Ciencias Físicas y Matemáticas, Universidad de Chile, Plaza Ercilla 803, Santiago, Chile
[2]Escuela de Geología, Facultad de Ingeniería, Universidad Santo Tomás, Ejército 146, Santiago, Chile
[3]Departamento de Ciencias Geológicas, Facultad de Ingeniería y Geología, Universidad Católica del Norte, Angamos 0610, Antofagasta, Chile
[4]Independent Tectonic Consultant
[5]Geología, Facultad de Ingeniería, Universidad Andrés Bello, Quillota 980, Viña del Mar, Chile

ABSTRACT

The Tarapacá Basin is one of the larger basins created on the western margin of South America during the Mesozoic times. Regional studies focused their attention on understanding its Cenozoic surface structures, traditionally interpreted as a west-verging thrust and fold belt. However, its internal and deep architecture and the influence of previously developed Mesozoic extensional structures on its current structure have not been analyzed in detail. We used new field data and 2D seismic data to determine the tectonic architecture of the Tarapacá Basin. We have paid special attention to defining both the deep and superficial structures to understand its tectonic evolution. The seismic data reveal the existence of a series of half-graben structures along which Mesozoic synrift stratigraphic sequences accumulated. We also show that Upper Cretaceous and Cenozoic synorogenic sequences mainly accumulated over contractional folds (anticlines and synclines). The structure is characterized by a thick-skinned structural style dominated by structures inverted during the oblique reactivation of ancient Mesozoic normal faults and also by newly formed reverse faults in the form of shortcut and bypass faults. The presence of Upper Cretaceous to Tertiary synorogenic sequences over the contractional structures, separated by angular unconformities, allowed us to show that the basin inversion and its subsequent deformation occurred at least since the Late Cretaceous until Recent times. These results aid in understanding the role of extensional structures in the evolution of orogenic belts and can be compared with similar structures around the world.

INTRODUCTION

The Central Andes is the largest active non-collisional mountain belt worldwide, located along the western margin of South America (Fig. 1). It is related to the subduction of the Nazca plate beneath the westernmost edge of South America, and its major topographic expression is observed along its curved portion in northern Chile and southern Peru and Bolivia (Fig. 1), where it reaches a width of nearly 450 km and a mean elevation of nearly 4 km above sea level (asl) along the so-called Altiplano-Puna plateau (Isacks, 1988). The western flank is mostly located on the Chilean side (Fig. 1). In northern Chile, between 18° and 22°S, this mountain belt is divided into four tectonic provinces: the Coastal Cordillera, the Central Depression, the Precordillera (or Domeyko Cordillera), and the Western Cordillera (Fig. 1).

The present-day tectonic configuration of the Central Andes (Fig. 1) has often been attributed to the almost continuous crustal shortening of the continental margin since at least ca. 90 Ma (Mpodozis and Ramos, 1989; Somoza, 1998; Farías et al., 2005; Mpodozis et al., 2005; Arriagada et al., 2006; Bascuñan et al., 2016, and others), associated with a major plate reorganization and changes in the relative velocity and convergence between Nazca and South America (Pardo-Casas and Molnar, 1987; Somoza, 1998). Nevertheless, its early tectonic history during the Mesozoic (Triassic–Jurassic–Early Cretaceous) was dominated by an extensional tectonic regime, characterized by the creation of different backarc extension related basins, and related to the retreating subduction, coeval with the breakup of the Pangea-Gondwana supercontinent (Coira et al., 1982; Mpodozis and Ramos, 1989, 2008; Franzese and Spalletti, 2001; Vicente, 2006; Ramos, 2010).

The Tarapacá Basin (Figs. 1 and 2) in northern Chile is one of the main basins that resulted from this Mesozoic extensional tectonic regime, which can be extended south toward the Copiapó region in Chile (27°S) and north toward southern Peru (Vicente, 2006). Its structural and stratigraphic relations have been mostly interpreted from field data in some sectors of the Domeyko Cordillera (Muñoz and Charrier, 1996; Ardill et al., 1998; Farías et al., 2005; Amilibia et al., 2008; Herrera et al., 2017), and also from seismic profiles of the Pampa del Tamarugal (Victor et al., 2004; Nester, 2008; Jordan et al., 2010; Nester and Jordan, 2012; Labbé et al., 2015) and the Salar de Atacama Basin (Pananont et al., 2004; Arriagada et al., 2006; Jordan et al., 2007, and others). Based on these studies, different structural styles have been recognized to affect both the infill and the basement of this basin. They are frequently related to thick-skinned thrust systems, strike-slip faults, and/or normal faulting (Mortimer, 1973; Flint et al., 1993; Muñoz and Charrier, 1996; Victor et al., 2004; Farías et al., 2005; Herrera et al., 2017). Despite these attempts, other regions of this basin are still unexplored. One of the main reasons for this gap is the presence

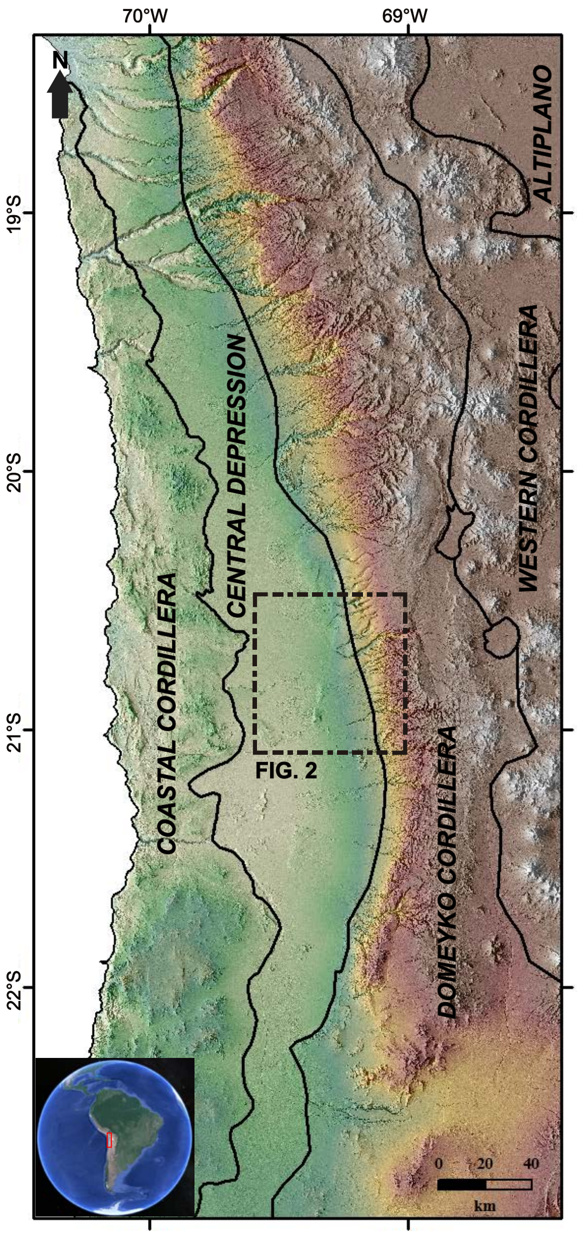

Figure 1. Digital elevation model (DEM) of northern Chile, along the normal subduction segment, showing the distribution of the main tectonic provinces. The black dashed square indicates the study area shown in Figure 2.

of thick Oligocene to Recent continental sequences (so-called "pampas") that almost completely cover the structures located along the Central Depression (Figs. 1 and 2), and therefore, structural studies in this region have mainly been oriented toward understanding Late Cenozoic deformation. As such, the complete structural configuration of the Taracapá Basin beneath the Central Depression and the western slope of the Precordillera (and/or Domeyko Cordillera) of the Central Andes at these latitudes is not yet understood (Figs. 1 and 2). Knowledge of these styles is essential to constraining future tectonic models and structural reconstructions.

In order to solve this problem and visualize the complete structure of the study region, we have carried out a structural interpretation of a series of W-E–oriented 2D seismic profiles located along the Pampa del Tamarugal in the central part of the Central Depression; these profiles highlight the subsurface structure. The seismic data are mainly constrained by field data and oil well data. In this contribution, we show for the first time the tectonic architecture of the Tarapacá Basin beneath the Pampa del Tamarugal in northern Chile.

GEOLOGICAL SETTING

Stratigraphy

The study area is located along the Central Depression (Figs. 1 and 2), between the Coastal Cordillera and the Domeyko Cordillera. In this region, the Pampa del Tamarugal occupies the central part of the Central Depression at 18°–22°S (Figs. 1 and 2). The oldest rocks lie well exposed in the southwest extreme of the study area and to the west of the Challacollo Hill (Fig. 2). These rocks consist of Upper Carboniferous intrusives that are mainly composed of granites and granodiorites (ca. 302 Ma; Sepúlveda et al., 2012), lithologically and chronologically correlated with those granitic blocks exposed along the Domeyko Cordillera and that correspond to the basement of the Tarapacá Basin (Fig. 2). The stratigraphic record of the basin is mostly exposed in the western part of the Domeyko Cordillera (Fig. 2) and also along some transverse canyons that cut the Pampa del Tamarugal. The infill is composed of Mesozoic and Cenozoic volcano-sedimentary deposits (Fig. 2). The Mesozoic deposits start with nearly 1640 m of sedimentary Upper Jurassic successions that unconformably overlie the Upper Carboniferous granitic rocks of the Domeyko Cordillera. These deposits are composed of intercalated siltstones, shales, and fine sandstones with *Perisphinctes* y *Arisphinctes* (Upper Oxfordian) defined as the Majala Formation (Galli-Olivier, 1967; Blanco et al., 2012), interpreted to have accumulated during extensional tectonic conditions (Mpodozis and Ramos, 2008). This unit is followed by a thick (~2000 m) continental succession of stratified red sandstones, mudstones, and siltstones. The tops of the beds frequently show traces of *ornithopods* of 60 × 50 cm scale, suggesting an Upper Jurassic–Lower Cretaceous age (Blanco et al., 2012). This unit corresponds to the Chacarillas Formation (Galli and Dingman, 1962; Blanco et al., 2012; Blanco and Tomlinson, 2013; Fig. 2),

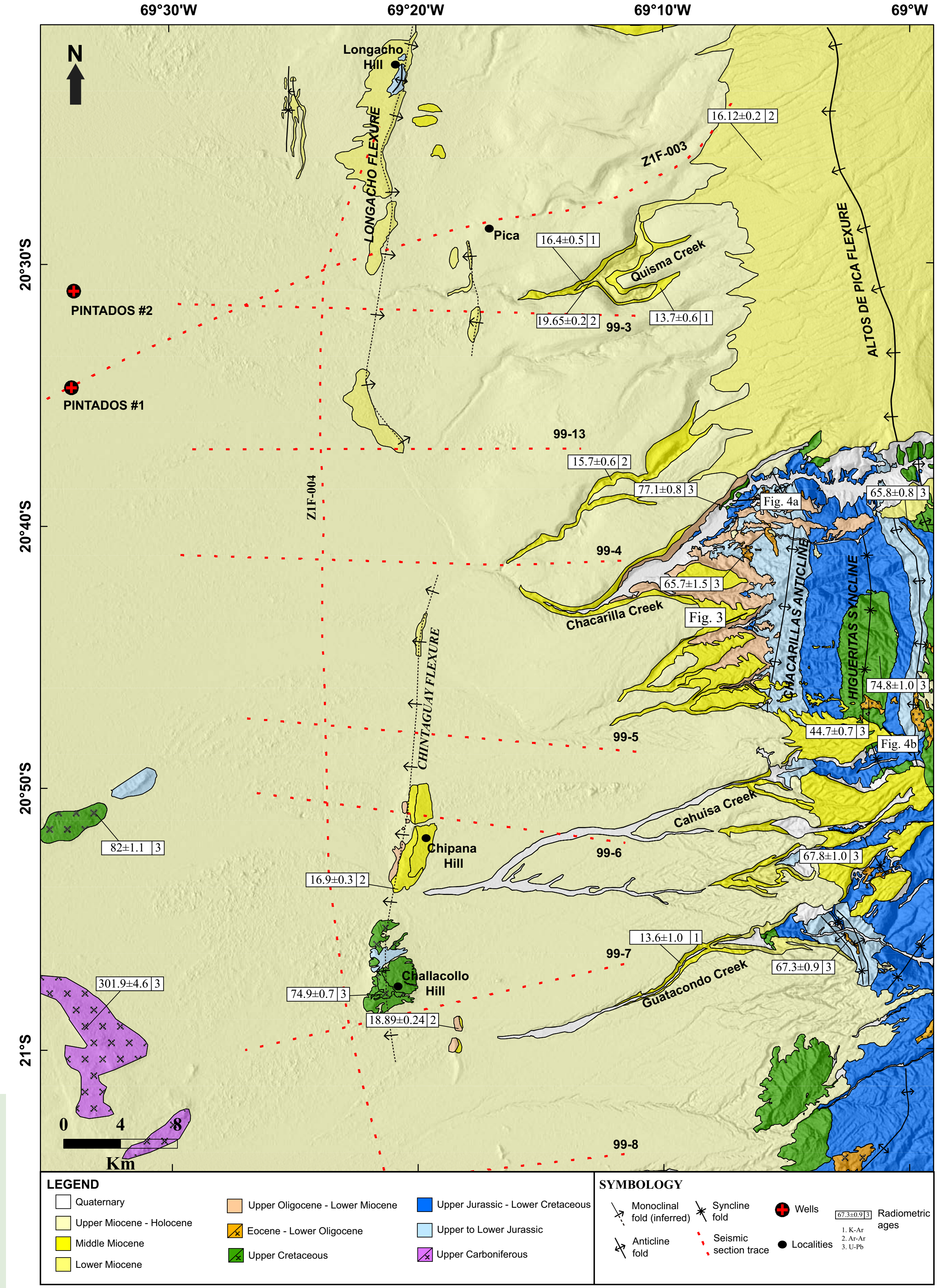

Figure 2. Simplified geologic map of the Tarapacá Basin along the Pampa del Tamarugal showing the main structural styles and geologic units exposed, as well as the distribution of the 2D seismic lines and boreholes used in this study. Modified from Tomlinson et al. (2001), Blanco et al. (2012), Sepúlveda et al. (2012), and Blanco and Tomlinson (2013).

which shows a notable west to east variation in thickness producing a wedge shape (Fuentes et al., 2016).

The Chacarillas Formation is unconformably covered by nearly 1400 m of Upper Cretaceous continental volcanic and sedimentary deposits made of conglomerates, sandstones, lavas, and tuffs associated with a volcanic arc setting (Galli and Dingman, 1962). These deposits are mostly exposed in the core of some syncline folds (e.g., Higueritas Syncline) and along isolated hills (e.g., Challacollo Hill) in the southern Pampa del Tamarugal (Fig. 2) and correlate with the Cerro Empexa Formation (Galli and Dingman, 1962; Blanco and Tomlinson, 2013). This succession usually exhibits contractional growth strata, especially over the frontal limbs of the anticline folds. U-Pb ages from volcanic zircons between 82.5 Ma and 68.2 Ma (Blanco et al., 2012), respectively, allow assignment of an Upper Cretaceous age to this unit.

All of these units (Majala, Challacollo, Chacarillas, and Cerro Empexa formations) are locally intruded by kilometer-scale Upper Cretaceous–Eocene (ca. 75–45 Ma) intrusive bodies (granodiorites, diorites, monzodiorites, etc.) along the axis of the folds (anticlines and synclines), located specifically in the western part of the Domeyko Cordillera (Fig. 2). The Cenozoic deposits consist of ~1700 m of Upper Oligocene to Middle Miocene deposits made of intercalations of sedimentary (sandstones and conglomerates) and volcanic (mainly tuffs) beds, which unconformably cover the Mesozoic and Upper Cretaceous outcrops of the westernmost part of the Domeyko Cordillera (Galli and Dingman, 1962; Galli-Olivier, 1967) (Figs. 2 and 3). These deposits are composed of the Altos de Pica Formation, which comprises mainly conglomerates and sandstones with intercalated ignimbrites with reported U-Pb ages of 19.6 Ma (Lower Miocene; Blanco et al., 2012) and the El Diablo Formation, which comprises sandstones, conglomerates, gravels, and some limestones (Galli and Dingman, 1962; Galli-Olivier, 1967; Tobar et al., 1968; Blanco et al., 2012), which underlie the extensive Plio-Pleistocene cover of the Pampa del Tamarugal (Fig. 2). The age of this formation is poorly constrained; however, we assigned a Mid-Upper Miocene age, based on its stratigraphic position. Finally, the Upper Miocene to Holocene sedimentary deposits are mostly distributed over the surface of the Pampa del Tamarugal, representing the youngest successions that complete the infill of the Tarapacá Basin (Fig. 2).

STRUCTURAL SETTING

The major surface of the Tarapacá Basin is covered by the Pampa del Tamarugal, which corresponds to a relatively flat surface showing a gradual eastward increase in altitude toward the Domeyko Cordillera (Figs. 1 and 2). This surface commonly prevents the observation of structural and stratigraphic relations in the region. However, the regional structure of the study area can be divided into two tectonic domains that form part of a large N-S–oriented contractional system (Muñoz and Sepúlveda, 1992; Muñoz and Charrier, 1996; Farías et al., 2005; Charrier et al. 2013; Herrera et al., 2017) (Fig. 2).

The eastern domain of this system is restricted to the westernmost part of the Domeyko Cordillera. At the study latitudes, it consists of large, N-S–

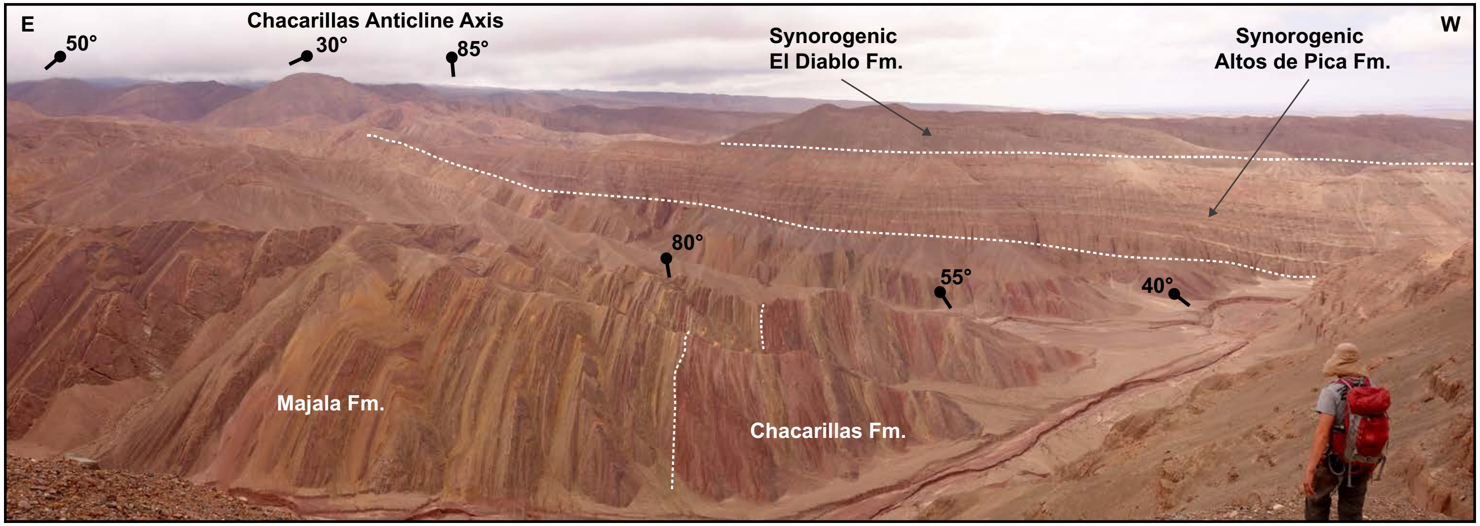

Figure 3. Panoramic view of the folded Jurassic–Cretaceous synrift successions (Chacarillas and Majala formations) into the Chacarillas Anticline (see location on Fig. 2), which are unconformably overlain by Oligo-Miocene synorogenic deposits (Altos de Pica and El Diablo formations).

striking, asymmetrical anticlines and synclines (e.g., Chacarillas Anticline; Figs. 2–4) that mainly involve the Jurassic–Lower Cretaceous deposits of the basin, forming a belt ~40 km long and 15 km wide, recognized as the northern expression of the Sierra de Moreno fold belt (Tomlinson et al., 2001) (Fig. 2). The folds are generally narrow, with tight to isoclinal geometries and steep limbs with dips that range between 50°–80°S (Figs. 3 and 4) (Blanco and Tomlinson, 2013). Previous works have associated these folds with west-verging blind thrusts (Amilibia and Skarmeta, 2003; Armijo et al., 2015), while others consider that they resulted from reactivated normal faults (Charrier et al., 2007; Fuentes et al., 2016; Herrera et al., 2017).

To the west and north of this sector, a second tectonic domain is present (Fig. 2). Here, the structural style is characterized by a series of NNW- to NNE-oriented flexures related to monoclinal folds, which are defined as the Altos de Pica, Longacho, and Chintaguay flexures (Fig. 2) and other minor open folds. These flexures and/or monoclinal folds have mostly been related to thick-skinned blind reverse faults (Pinto et al., 2004; Victor et al., 2004; Nester, 2008; Blanco et al., 2012; Charrier et al., 2013; Fuentes et al., 2016; Fuentes et al., 2017). Some of these (Altos de Pica flexure) have been used to explain the structure of the western region of the Altiplano (Victor et al., 2004; Farías et al., 2005; Charrier et al., 2013). In addition, other large west- and east-verging reverse faults that extend from the Longacho Hill to the south of the Guatacondo Creek have been interpreted based on previous analysis of seismic and field data (Victor et al., 2004; Nester, 2008; Jordan et al., 2010; Nester and Jordan, 2012; Labbé et al., 2015). Many of these were interpreted as inverted faults (Charrier et al., 2013; Fuentes et al., 2016; Fuentes et al., 2017; Herrera et al., 2017), because these bound the lateral continuity of the Mesozoic deposits related to the synrift infill of the Tarapacá Basin (Gallardo, 2015; Fuentes et al., 2016; Fuentes et al., 2017). In map view, all these structures (reverse and inverted faults) can be seen affecting the Oligocene and Neogene volcanic and sedimentary deposits, and also the oldest Mesozoic deposits (Fig. 2). Previous works (Muñoz and Charrier, 1996; Pinto et al., 2004; Victor et al., 2004; Farías et al., 2005; Jordan et al., 2010; Charrier et al., 2013) have described this structural array as responsible for the accommodation of major deformation and uplift of the western slope of the Central Andes at least during the past ~28 m.y. (Farías et al., 2005; Cortés et al., 2012). Previous estimates suggest that both tectonic domains could have accumulated between 30 and 50 km of shortening (Armijo et al., 2015) along the Guatacondo Creek (Fig. 2). In contrast, other works indicate that the accumulated horizontal shortening by these structures does not exceed 10 km (Haschke and Günther, 2003; García and Hérail, 2005; Herrera et al., 2017).

METHODOLOGY

Field Data

We constructed a geologic map (1:100,000 scale; Fig. 2). This process was supported by the use of satellite images, direct field observations, and structural measurements (strike and dip) of the geologic structures. Our observations aimed to identify structural and stratigraphic relations, such as contacts between stratigraphic units, variations in thickness along successions, the presence of intra-formational faults, angular unconformities, synextensional and synorogenic deposits, and the determination of the vergence of faults and folds, among other features.

2D Seismic Data

In order to understand the structure of the Tarapacá Basin beneath the Pampa del Tamarugal, we used a series of W-E–oriented seismic profiles (more than 100 km) (lines 99-3–99-6; Fig. 2), corresponding to a two-dimensional (2D) seismic survey acquired by Evergreen Resources and Empresa Nacional del Petróleo (ENAP) during 1999 to explore oil and gas opportunities along northern Chile. The seismic acquisition was made using explosives and a receiver system composed of 12 geophones with a nominal frequency of 10 Hz. The seismic profiles typically have good vertical and lateral resolution. During processing, the profiles were filtered and migrated in time, and therefore the vertical scale used is in seconds (two-way traveltime [TWT]). Unfortunately, the time-depth conversion of the seismic data was not performed, due to the absence of density information, sonic and check shots, or logs from the boreholes Pintados 1 and 2 (Fig. 2), which are necessary to perform this conversion.

Seismic and Structural Interpretation

The seismic data were mostly constrained by geological information derived from the exposures of the westernmost part of the Domeyko Cordillera and also by information available (stratigraphy and lithology) from the boreholes Pintados 1 and 2, located west of the study area (Fig. 2). To carry out the seismic and structural interpretation, first, we identified the first-order unconformities to define and separate the main tectonosequences related to the infill of the basin. Afterwards, the surface geological information (mainly geologic contacts) was projected into the seismic profiles, and the main seismic reflectors were correlated with those units exposed on the surface. The stratigraphic information from the Pintados boreholes, related to the position of the geologic units in the subsurface, was also correlated with the main seismic reflectors and between the different seismic profiles. The geologic structures (faults and folds) were determined based on the following criteria: lateral loss and break of seismic reflectors, drastic changes in dip of seismic reflectors, presence of truncated seismic reflectors, lateral changes of seismic amplitudes, etc. The seismic visualization, interpretation, and the individual modeling of faults and folds were made using the StructureSolver software and the Andino 3D software of La. Te. Andes S.A. The individual modeling of faults and folds consisted of interactively changing the geometry (mainly the shape of the fault planes), kinematic parameters (slip, propagation rate, etc.), and mode of deformation

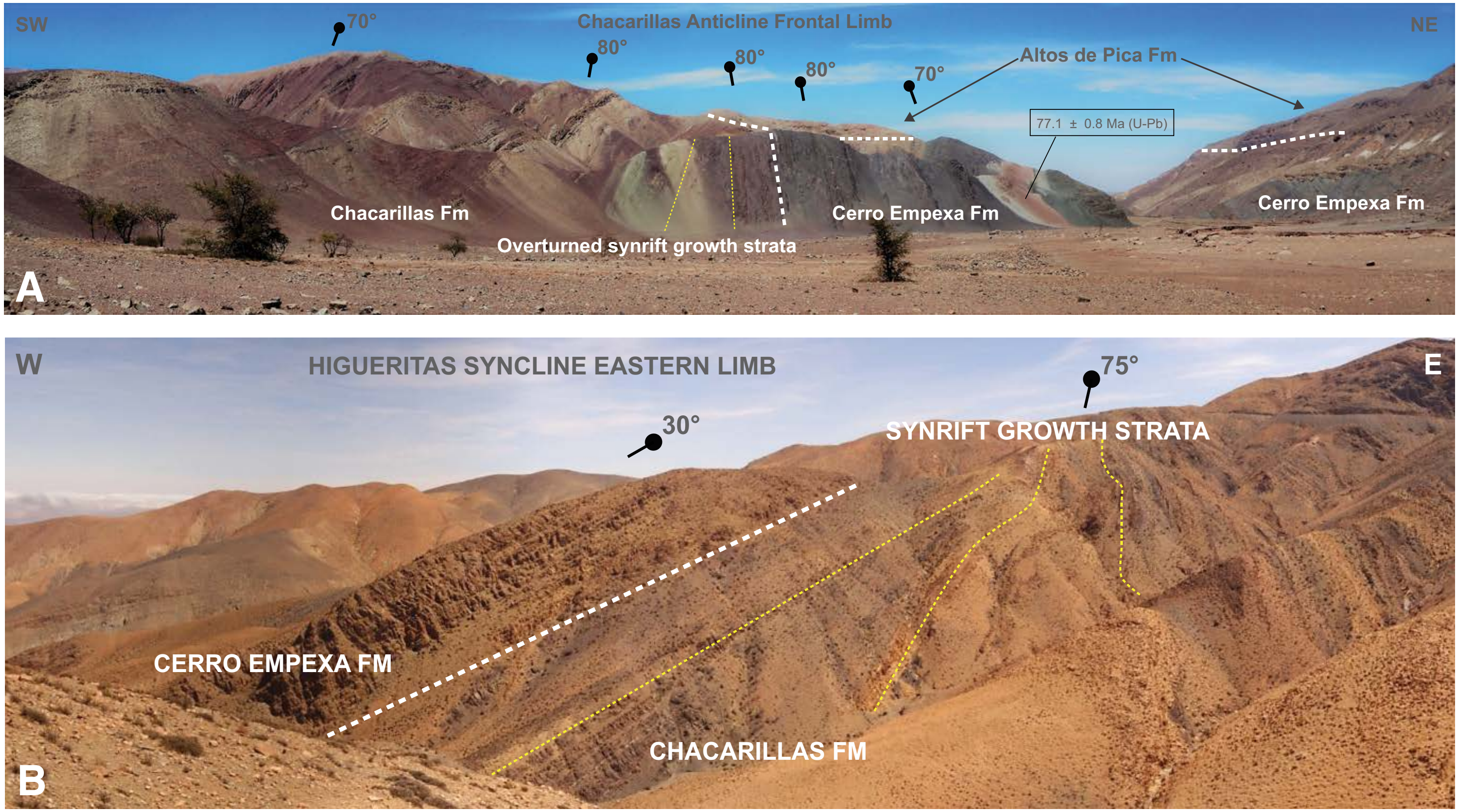

Figure 4. (A) View of the steeply inclined frontal limb of the Chacarillas Anticline involving the Jurassic–Lower Cretaceous synrift successions of the Chacarillas Formation in contact with the Upper Cretaceous synorogenic successions of the Cerro Empexa Formation (see location on Fig. 2). (B) Partial and transversal view of the eastern limb of the Higueritas Syncline. Note the contact between the Jurassic–Cretaceous synrift deposits of the Chacarillas Formation and the Upper Cretaceous synorogenic sequences of the Cerro Empexa Formation (see location in Fig. 2).

(trishear, flexural slip, flexural flow, simple shear, etc.) of the structures until these have matched the observed structures in the field and seismic profiles. This process inherently restricts deformation to two dimensions.

RESULTS

Major Stratigraphic Tectonosequences

The analysis of the lateral and vertical variations of the seismic reflectors and the identification of angular unconformities and seismic-reflection terminations, e.g., downlaps, onlaps, and erosional truncations (Mitchum et al., 1977; Vail et al., 1977), allowed us to identify six major tectonosequences overlying the acoustic basement. Considering their geometries and structural and stratigraphic relations, we separated these into two types: synrift and synorogenic tectonosequences (Fig. 5), each one identified with a number (e.g., TS1, TS2, etc.) according to their positions in the geological record. The lithological characteristics of these are described in Geological Setting. The ages of the tectonosequences were assigned based on their fossil content and a few radiometric ages determined from samples from outcrops and the Pintados wells (Galli and Dignman, 1962; Tomlinson et al., 2001; Blanco et al., 2012; Blanco and Tomlinson, 2013; see Geological Setting). Also, we considered previous stratigraphic correlations presented in oil exploration reports of the Tarapacá Basin (Gallardo, 1961). Below, we describe each of them.

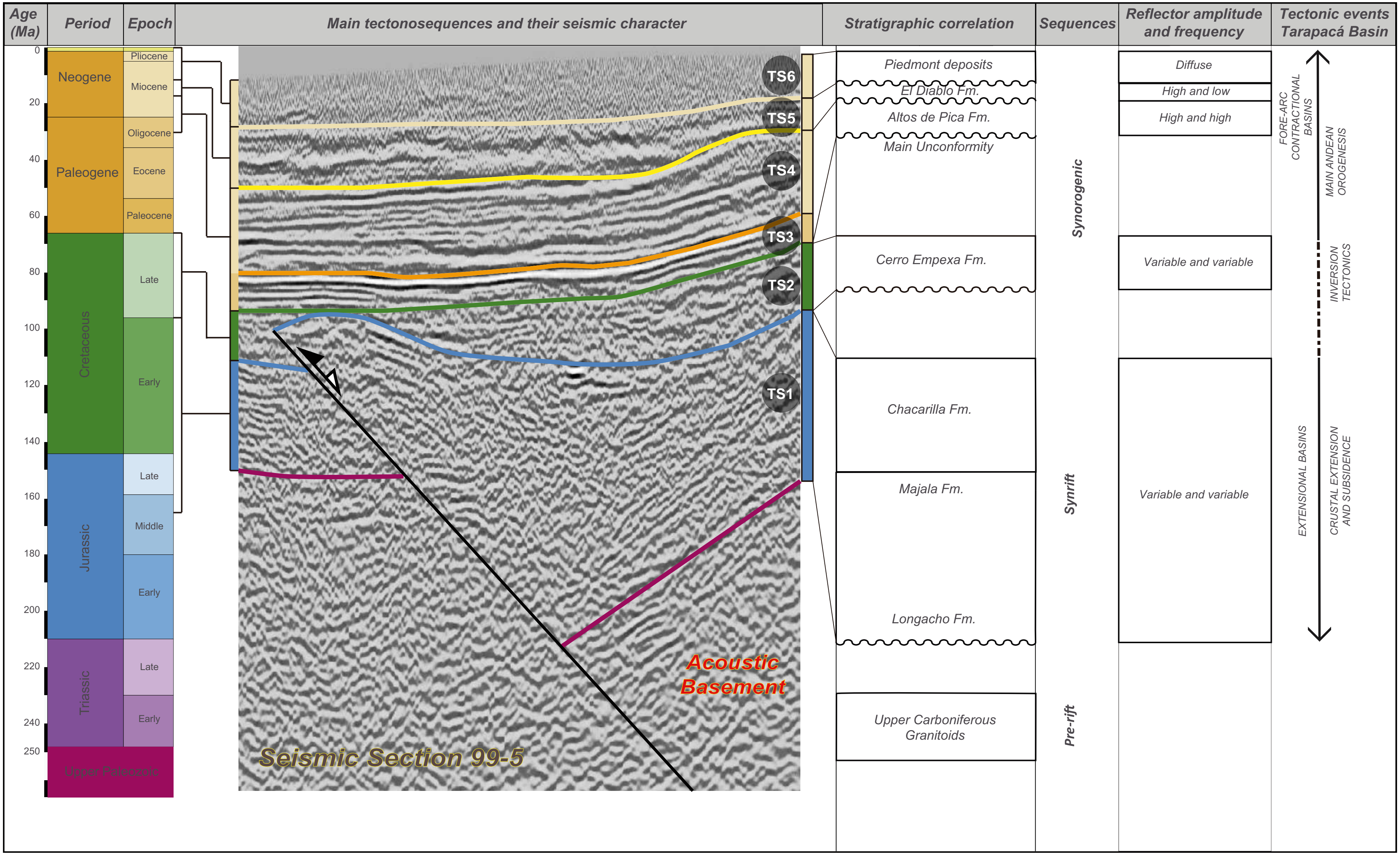

Figure 5. Correlation template between the geologic units exposed on the surface and the main tectonosequences identified from the seismic-reflection data.

Basement

The basement commonly is characterized by a series of chaotic seismic reflectors (Fig. 5) that correspond to the acoustic basement. This basement is mainly related to the Paleozoic granitic rocks that form the pre-rift basement of the Tarapacá Basin (see Geological Setting). Its top is frequently marked by a continuous seismic reflector with high amplitude (Fig. 5) that can be traced along the entire seismic profile. This seismic reflector forms a regional angular unconformity that separates the basement from the oldest stratified successions.

Tectonosequence 1 (TS1)

This is the oldest stratigraphic tectonosequence and consists of semicontinuous and continuous seismic reflectors with variable amplitude (Fig. 5). Their basal seismic reflectors frequently show onlap terminations against the top of the basement, defining thus an angular unconformity. The complete package of reflectors has a wedge shape that thickens toward fault planes (Fig. 5), with a geometry similar to those reported for synrift deposits accumulated in the hanging walls of normal faults. Based on its geometry and stratigraphic position observed both at the surface and in the subsurface, we have interpreted this tectonosequence to be synrift deposits correlated with the Jurassic and Lower Cretaceous deposits of the Majala and Chacarillas formations (Fig. 5).

Tectonosequence 2 (TS2)

This sequence is composed of a package of semicontinuous seismic reflectors (with variable frequency) that commonly have onlap terminations against the top of the underlying TS1 (Fig. 5). This unit has important variations in thickness, different from those observed in TS1. The basal seismic reflectors are frequently more inclined than the upper reflectors, forming a fan shape. Growth strata geometries are generally thicker over the limbs of anticline and syncline cores and are very well exposed toward the eastern parts of lines 99-3 (Fig. 6), 99-4 (Fig. 7), and 99-5 (Fig. 8). We have correlated this tectonosequence with the Upper Cretaceous synorogenic deposits of the Cerro Empexa Formation (Fig. 5), exposed along the Challacollo Hill (Fig. 2). Correlation with Cretaceous volcanic sequences was also previously made from the Pintados oil wells (Gallardo, 1961; Mordojovich, 1965).

Tectonosequence 3 (TS3)

This sequence corresponds to a thin package of parallel and continuous seismic reflectors with high amplitude (Fig. 5). Its lower section is marked by a prominent angular unconformity that separates this tectonosequence from the underlying TS2 and TS1 (Fig. 5). The parallel seismic reflectors that compose this tectonosequence commonly thin toward the limbs of anticline and syncline folds, showing geometries related to growth strata (Figs. 5 and 6). Following the stratigraphic record recognized in the western flank of the Domeyko Cordillera, we have correlated this tectonosequence with the synorogenic Upper Oligocene–Lower Miocene deposits of the lower section of the Altos de Pica Formation (Fig. 5).

Tectonosequence 4 (TS4)

This is a thick package of parallel and continuous seismic reflectors with intercalated high and low amplitudes (Fig. 5). The unit is separated from the underlying TS3 by a gentle angular unconformity, which is frequently marked by a basal seismic reflector of high amplitude (Fig. 5). Similar to TS3, this tectonosequence in some places shows asymmetric fan geometries, especially over the limbs of some folded structures, thus indicating a contemporary accumulation during contractional deformation. The strata thickness generally increases toward the western side of the Pampa del Tamarugal. The top of this tectonosequence is correlated with the top of the upper section of the Altos de Pica Formation exposed in the western Domeyko Cordillera, and, therefore, we interpret this tectonosequence as the upper Altos de Pica Formation (Lower Miocene).

Tectonosequence 5 (TS5)

This sequence unconformably overlies TS4 and consists of a series of parallel and semicontinuous reflectors with high amplitude and low frequency (Fig. 5). This unit commonly is wedge shaped, with thinning toward the frontal limbs, over the crest of the inversion anticlines and/or other contractional structures (Figs. 6, 8, and 9). This geometry usually is acquired when contractional deformation and sedimentation occur simultaneously at different rates. Based on these observations, we interpreted the unit as a synorogenic tectonosequence, which can be correlated with the Miocene El Diablo Formation.

Tectonosequence 6 (TS6)

This sequence represents the youngest succession within the Tarapacá Basin. It consists of a reflector package that has diffuse amplitude and frequency (Fig. 5) and covers the complete stratigraphic record. On the surface, it is composed of semiconsolidated and unconsolidated sediments that form the Pampa del Tamarugal. Based on the stratigraphic correlations of the Upper Cenozoic deposits in the region, we have interpreted this tectonosequence as the Upper Miocene–Recent piedmonts deposits (Fig. 5). This tectonosequence is also seen to be affected by contractional deformation, and, therefore, we consider it the youngest synorogenic succession accumulated in the basin.

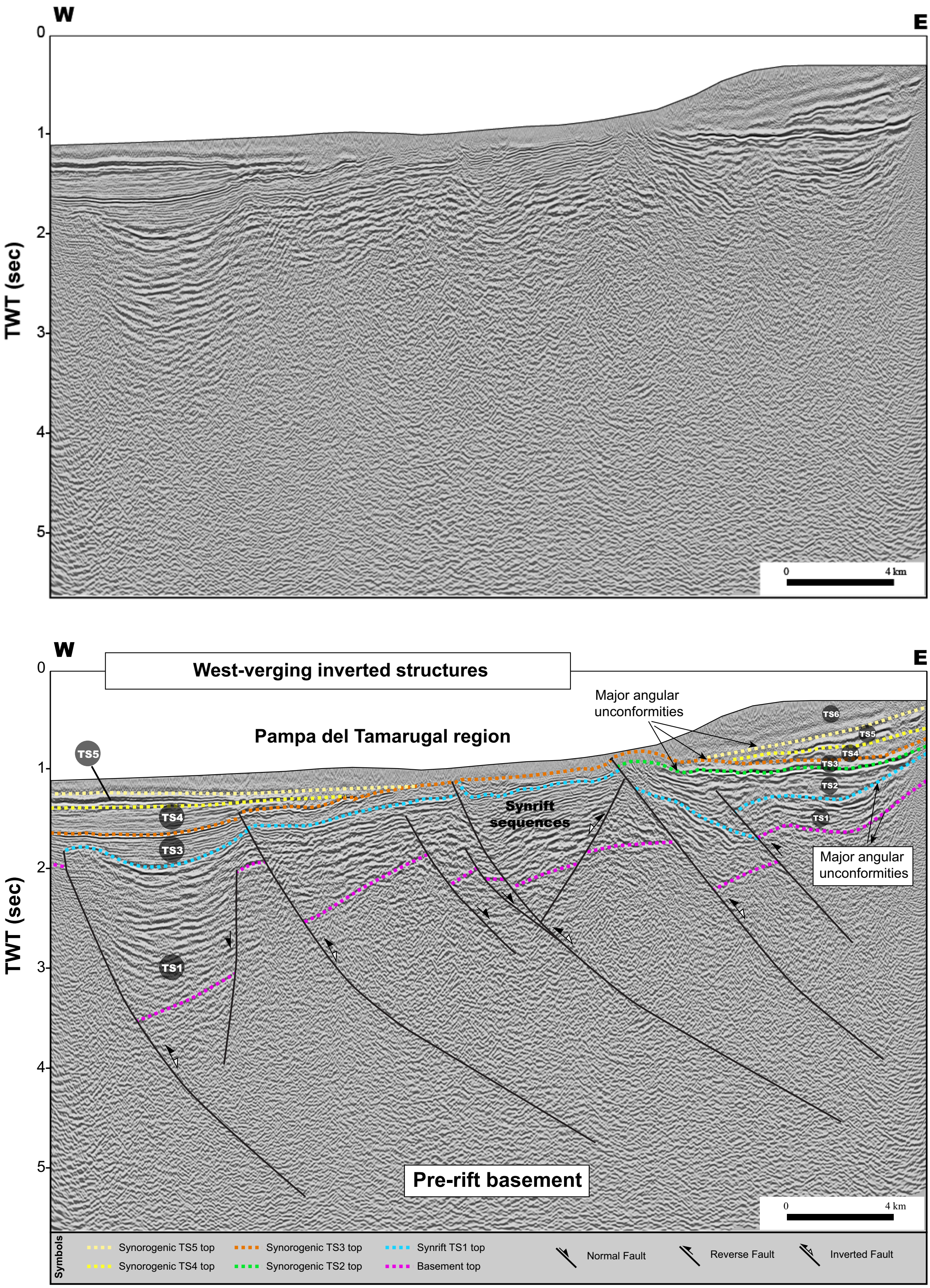

Figure 6. Representative 2D seismic profile 99-3 showing the different inverted half-graben structures interpreted along the northern part of the Pampa del Tamarugal. For location of the seismic profile, see Figure 2. TWT—two-way traveltime.

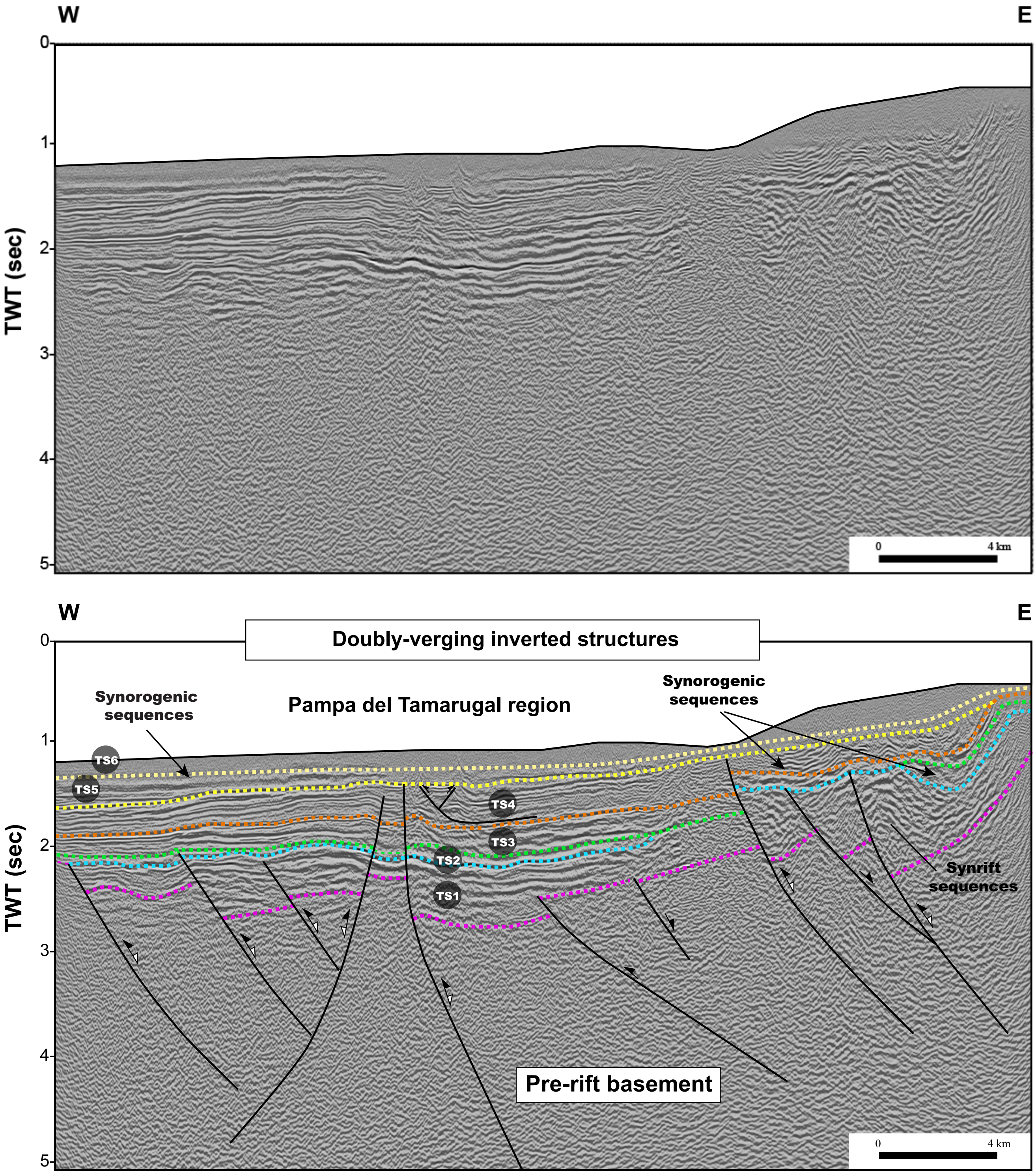

Figure 7. Representative 2D seismic profile 99-4 showing the preferably west-vergent inverted structures interpreted along the central part of the Pampa del Tamarugal. For location of the seismic profile, see Figure 2. Same symbols as in Figure 6. TWT—two-way traveltime.

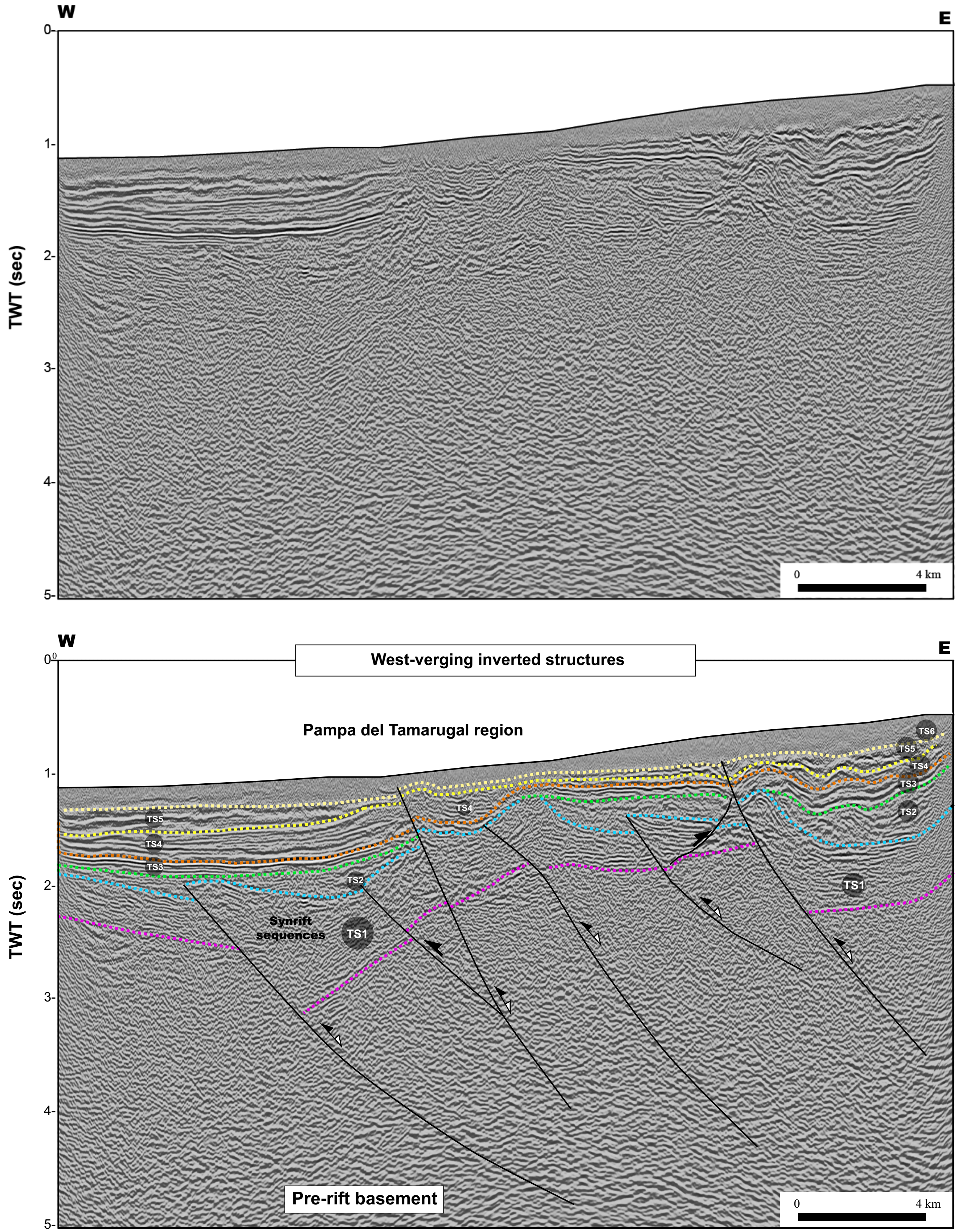

Figure 8. Representative 2D seismic profile 99-5 showing the main inversion anticlines related to reactivated Mesozoic normal faults along the central part of the Pampa del Tamarugal. For location of the seismic profile, see Figure 2. Same symbols as in Figure 6. TWT—two-way traveltime.

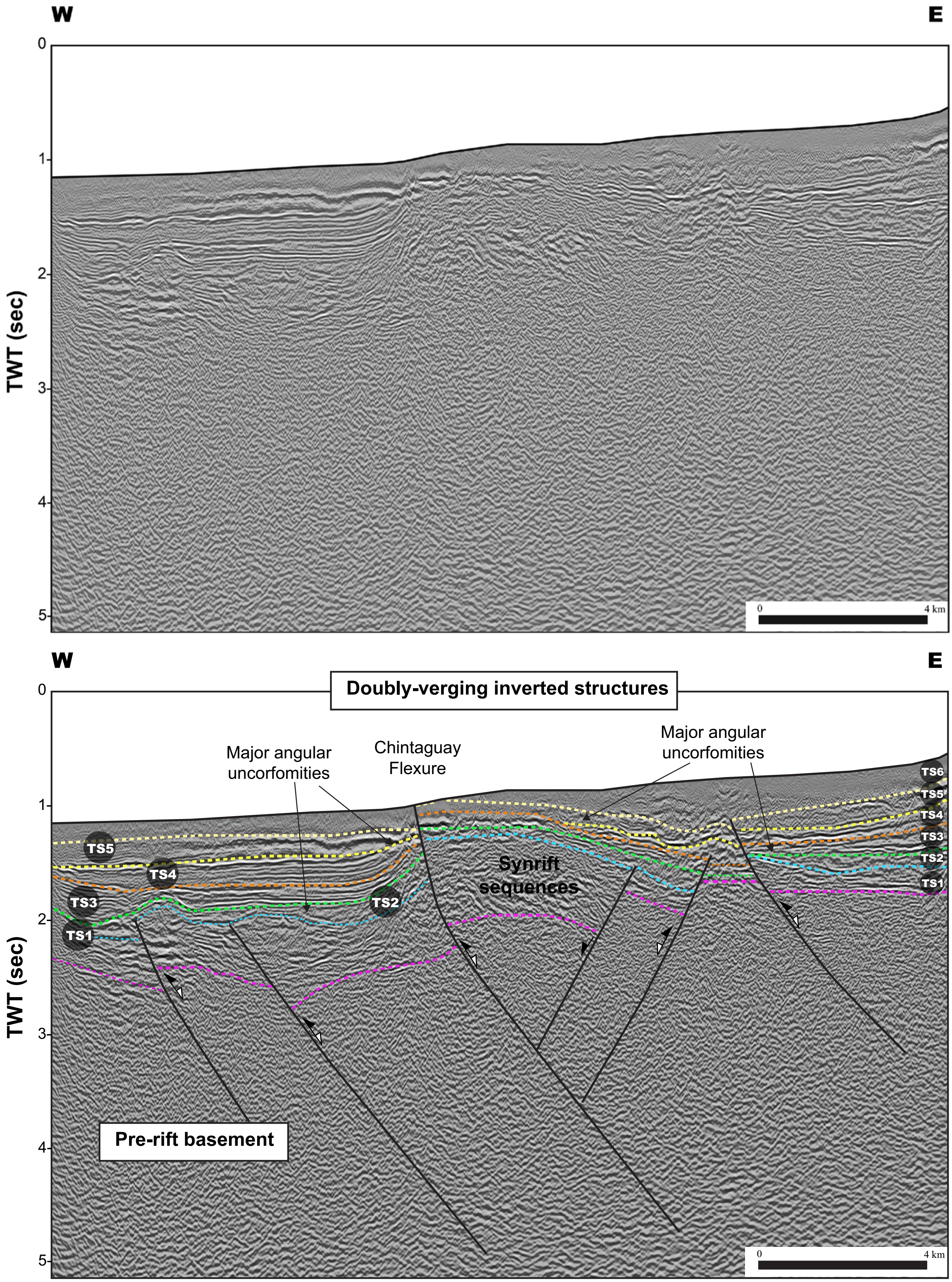

Figure 9. Representative 2D seismic profile 99-6 showing the doubly-vergent inverted folds and faults mostly identified along the southern part of the Pampa del Tamarugal. For location of the seismic profile, see Figure 2. Same symbols as in Figure 6. TWT—two-way traveltime.

STRUCTURE AND ARCHITECTURE OF THE TARAPACÁ BASIN

The seismic and structural interpretation of the W-E–oriented seismic profiles (Fig. 2) reveals that the structure of the basin is composed of two main basement-involved structural styles—inverted faults and folds and reverse faults. These styles commonly show along-strike variations in terms of geometry and kinematics, which are mostly related to the original pre-orogenic configuration of the basin inherited from previous extensional deformation episodes. Other subsidiary and minor faults are also identified; however, these have not greatly influenced the regional structure.

The major faults consist of steep to moderately dipping (50°–80°) doubly verging faults (Figs. 6–9) that commonly penetrate into the crystalline basement, with fault planes that vary between planar and semi-listric (Figs. 6–9). The central and easternmost faults usually affect the complete Mesozoic and Cenozoic tectonosequences (TS1–TS6), and in some cases, reach the surface (e.g., Challacollo Hill; Figs. 6 and 8) and define the modern western deformation front of the Domeyko Cordillera. Usually these faults have steep dips that exceed 50°. This geometric relationship is similar to those reported in strike-slip fault zones; however, the seismic data in hand are inadequate to distinguish between the two possibilities. Thus, an oblique kinematics dominated by dip and strike slips is possible. The westernmost faults mainly are buried under the TS3–TS6 tectonosequences (Figs. 6–9). These faults bound a number of Mesozoic depocenters and/or en echelon half-graben structures, along which the Mesozoic synrift deposits (TS1) were preferably accumulated.

The hanging walls of the faults mostly consist of west-verging anticlines that involve the synrift stratigraphic wedges of TS1 (Figs. 6–9), except in the western and central segments of seismic lines 99-4 (Fig. 7) and 99-6 (Fig. 9), where the structural array is clearly doubly verging. The folds are asymmetric, with short and steep frontal limbs and large and less inclined back limbs (Figs. 6–9). They show a harpoon-shaped anticline facing toward the footwall faults, and some display evidence of buttressing against the faults (Figs. 6–8). These structures are well preserved along different sectors of the basin (Figs. 6–8) and correspond to large reactivated Mesozoic master faults. This geometry frequently is acquired when previously formed high-angle normal faults are partially reactivated and asymmetrical synrift stratigraphic wedges are folded.

In the central part of the basin, some of the hanging-wall and footwall fault blocks are displaced by subsidiary short-cut and bypass faults, along which the top of the basement is uplifted and folded. The short-cut faults consist of minor upward splays with reverse slip motion, linked to reactivated Mesozoic normal faults that affect their footwall (Figs. 6 and 8). The bypass faults consist of reverse faults that affect the hanging wall of the Mesozoic reactivated normal faults. Based on the structural and stratigraphic relations mentioned above, we interpreted that the structure of the basin is mainly dominated by structural styles (inverted faults, inversion anticlines, and reverse faults) associated with the tectonic inversion of ancient Mesozoic normal faults.

The seismic resolution generally did not allow determination of the position of the basal detachment of these structures. However, based on the geometry and displacement of the master faults, we believe that these sole into a deep basal detachment that could be located outside the footprint of the seismic data (below 5 s TWT). The seismic profiles also show the presence of thick and asymmetrical stratigraphic wedges that unconformably cover both the inversion anticlines and the hanging walls and footwalls of reverse faults (Figs. 6–9). These wedges are composed of Upper Cretaceous (TS2) and Cenozoic tectonosequences (TS3–TS6) and have stratigraphic geometries similar to those related to synorogenic sequences (Vergés et al., 2002). The basal sections of these units usually onlap against the limbs of the inversion anticlines, forming a clear angular unconformity that marks the initial pulses of the tectonic inversion of ancient Mesozoic normal faults (Fig. 6–9). Other angular unconformities are also identified internally within these stratigraphic wedges, which have recorded other younger Cenozoic contractional pulses (Figs. 6–8).

DISCUSSIONS

Influence of Inherited Structures

The present-day tectonic architecture of the Tarapacá Basin in the Pampa del Tamarugal region has been usually related to Neogene shortening of the continental margin, mostly accumulated in the Domeyko Cordillera and the Western Cordillera, along the Chilean side. In a continental context, some works have suggested that this region forms part of a west-verging hybrid (thin- and thick-skinned) fold-and-thrust belt composed of imbricated folds and thrust faults developed 50 m.y. ago (Armijo et al., 2015). In contrast, the seismic data used in this work have revealed that the structure of this region is mostly related to a thick-skinned contractional system, as was indicated earlier by Victor et al. (2004) and Nester (2008).

Our structural and seismic interpretation shows that the vergence of this system is conditioned by the initial polarity of ancient preexisting basement structures, which are commonly susceptible to being reactivated when a contractional deformation is superimposed (Martínez et al., 2017). Our results also indicate that the current contractional structures beneath the Pampa del Tamarugal region are geometrically and kinematically related to the tectonic inversion of west- and east-inclined basement normal faults (Fig. 8) inherited from Jurassic–Early Cretaceous extensional episodes (Mpodozis and Ramos, 2008). Similar structural styles have been recognized in the Cordillera de Domeyko (Amilibia et al., 2008) and along other regions such as the Cordillera Oriental and the Salta Rift on the Argentinean side of the Andes (Kley et al., 1999; Kley and Monaldi, 2002; Carrera et al., 2006; Iaffa et al., 2011, and others). In the latter, the major folds and faults also are usually associated with the positive reactivation of previous Jurassic–Early Cretaceous normal faults and other zones of weakness within the basement rocks.

The structural elements commonly observed in the study area correspond to large and asymmetrical inversion anticlines, reactivated normal faults, and basement reverse faults (Fig. 10). Other structural styles linked to hybrid (thin-

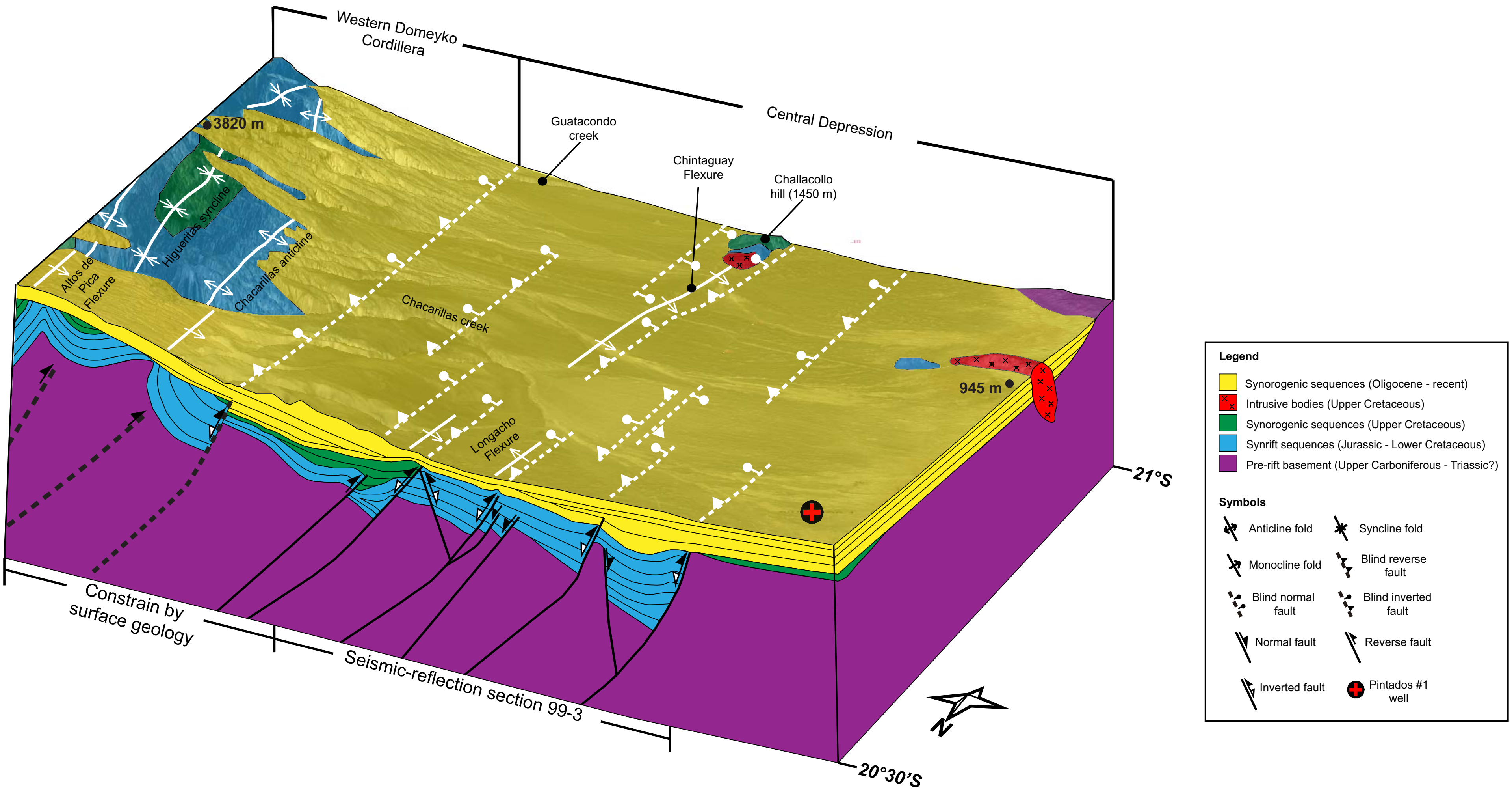

Figure 10. 3D schematic model of the regional structure of the Tarapacá Basin along the Pampa del Tamarugal, constructed over the interpretation of the 2D seismic profiles. The hypothetical deep structure was constructed assuming the continuity of the fold belt exposed south of Chacarillas creek.

and thick-skinned) thrust ramps previously proposed for this region (Amibilia and Skarmeta, 2003; Armijo et al., 2015) are not observed, and their continuity in the lower sections of the upper crust is not evident from the seismic data. We interpret that the west-verging folds and faults observed in the field are strongly controlled by the initial dip of previous normal faults (Figs. 7–10), which were later reactivated forming inversion anticlines at their hanging-wall blocks.

Some of these inversion anticlines have narrow and pop-up geometries associated with high-angle faults (Fig. 8), similar to those observed in deformation zones related to strike-slip faults. Based on this, we do not rule out that part of the deformation experienced during tectonic inversion has been accommodated by strike-slip motion. The situation usually occurs when normal faults and the over-imposed contractional stress field ($\sigma1$) are relatively oblique (Lowell, 1995; Bonini et al., 2012), or when previously developed normal faults have steep dips, thus allowing an oblique reactivation during their contraction. Some previous works (Farías et al., 2005) have suggested that part of the shortening experiment by the westernmost part of the Domeyko Cordillera is accommodated by strike-slip deformation. A right-lateral motion also was confirmed from the focal mechanisms related to the Aroma earthquake in 2001 (Legrand et al., 2007).

Similar to the interpretation of Farías et al. (2005), we note that the N-S–oriented monocline folds exposed in this region correspond to first-order structures that resulted from repeated positive reactivation of ancient basement normal faults (Fig. 10) and that the strike-slip motions recorded by the focal mechanisms only accommodated the regional contractional deformation. The monocline folds observed in the field are located over some of the inversion anticlines determined from the 2D seismic profiles. This relationship is given because the monocline folds usually affect synorogenic deposits (Fig. 3), which acquire a different geometry during basin contraction. This structural relationship has been observed in other deformed belts dominated by inverted structures (e.g., the eastern Coastal Cordillera of Chile, the Cordillera Oriental de Colombia, the Anti-Atlas of Morocco, and others) and also reproduced by sandbox analogue models (Mitra, 1993; Yamada and McClay, 2004).

Episodes of Deformation

Extensional deformation is frequently recognized due to the occurrence of synrift sequences (TS1) accumulated in the hanging-wall blocks of partially reactivated Mesozoic (Jurassic to Early Cretaceous) normal faults. These faults represent stratigraphic evidence that marks the initial opening of the half grabens that formed the Tarapacá Basin during the Jurassic, as proposed by Mpodozis and Ramos (1989, 2008). The stratigraphic wedges and growth strata of the synorogenic deposits over the crest, fore, and/or back limbs of the inverted contractional structures record the progressive structural evolution of the study area. The angular unconformity between TS1 and TS2 (Cerro Empexa Formation) suggest that Andean deformation in the region started as early as Late Cretaceous and was mainly accommodated by the oblique reactivation of Mesozoic normal faults (Fig. 10). This interpretation coincides with some previous studies carried out in nearby regions, such as the Salar de Atacama Basin, Cordillera de Domeyko, the Coastal Cordillera, and even in the Frontal Cordillera (Mpodozis et al., 2005; Amilibia et al., 2008; Martínez et al., 2013, 2016; Bascuñan et al., 2016; López et al., 2017, and others), where this period has been interpreted as the oldest deformation episode of the western Central Andes, associated with the "Peruvian" tectonic phase (Steinmann, 1929), which was responsible for the tectonic inversion of previous Triassic, Jurassic, and Early Cretaceous rift basins. Based on this interpretation, we recommend taking into consideration this older deformational episode when reviewing some of the proposed tectonic restorations (Farías et al., 2005; Arriagada et al., 2008; Armijo et al., 2015; Herrera et al., 2017).

The deformed tectonosequences correlated with the Oligocene to Mio-Pliocene deposits usually are separated by folded angular unconformities, thus indicating that other contractional pulses occurred from the Oligocene to Recent times. Commonly, tectonosequences TS3–TS6 fill asymmetrical contractional basins located in the footwall of reverse and inverted faults. These tectonosequences display geometries similar to those recorded by synorogenic deposits accumulated during progressive limb rotation of folded structures (Hardy and Poblet, 1994). Another important tectonic pulse has been commonly interpreted to occur during the Eocene; it is named the "Incaic" tectonic phase (Steinmman, 1929; Mégard, 1984; Maksaev and Zentilli, 1999, Charrier et al., 2009) and was responsible for the uplift of the Domeyko Cordillera east of the study area. In this study, we have not recognized synorogenic deposits related to this episode. The presence of Cenozoic (Oligocene to Recent) synorogenic deposits over the oldest Upper Cretaceous synorogenic sequences of the Cerro Empexa Formation also indicates that, during the Cenozoic, the previously inverted Mesozoic normal faults were once again reactivated. Considering the thickness of the Cenozoic tectonosequences, we interpret that the Pampa del Tamarugal region experienced major mechanical subsidence related to contractional deformation and uplift of basement blocks during these periods (Oligocene to Recent).

CONCLUSIONS

The tectonic architecture of the Tarapacá Basin between the Coastal Cordillera and the Domeyko Range consists of a preferentially west-verging contractional system, with some east-verging structures. The seismic and structural interpretation of 2D seismic profiles suggests that this region is mainly characterized by a thick-skinned structural style, dominated by inverted structures and basement-involved reverse faults. The tectonosequences that infill the basin beneath the Pampa del Tamarugal commonly correspond to Mesozoic synrift deposits and Upper Cretaceous to Cenozoic synorogenic deposits, which have recorded the different episodes of shortening and uplift of the Central Andes of northern Chile. The Andean deformation was mostly concentrated along reactivated normal faults that form part of ancient half-graben structures, creating thus large inversion anticlines, short-cut faults, etc. The tectonic vergence usually is controlled by the initial polarity of the Mesozoic normal faults. Their tectonic reactivation commonly formed large inversion anticlines with a structural style different from a classical thrust and fold belt. These structures frequently form monocline flexures on the surface exposed along the western edge of Domeyko Cordillera and the Central Depression of northern Chile (18°–22°S). The structural and stratigraphic relationships observed along the region allowed the determination of three main tectonic episodes: (1) Late Jurassic–Early Cretaceous extension related to the opening of the Tarapacá Basin; (2) Late Cretaceous contractional deformation, which produced the initial tectonic inversion of the Tarapacá Basin; and (3) Oligo-Recent contractional deformation associated with western Andean uplift. The structural style interpreted in this work shows the influence of pre-orogenic structures during the growth of an orogenic belt; this interpretation can be compared with analogue cases worldwide.

ACKNOWLEDGMENTS

We gratefully acknowledge the Empresa Nacional del Petróleo (ENAP) for permission to use seismic-reflection profiles and well data. The first author is thankful for financial support provided by the Comisión Nacional de Investigación Científica y Tecnológica (CONICYT) program through a Ph.D. scholarship. We thank D. Carrizo and the Advanced Mining Technology Center (AMTC; Universidad de Chile) for funding the first field trip campaigns to Domeyko Cordillera. La.Te. Andes S.A. and Nunns and Rogan LLC kindly provided us the Andino 3D software and StructureSolver software, respectively. We truly thank Antonio Díaz for assistance in the field. Finally, we thank Science Editor Raymond Russo and one anonymous reviewer for their valuable comments, which helped to improve the previous version of this manuscript.

REFERENCES CITED

Amilibia, A., and Skarmeta, J., 2003, La inversión tectónica en la Cordillera de Domeyko en el norte de Chile y su relación con la intrusión de sistemas porfíricos de Cu-Mo: X Congreso Geológico Chileno, Concepción, Resumen Extendido, v. 2, p. 1–7.

Amilibia, A., Sàbat, F., McClay, K.R., Muñoz, J.A., Roca, E., and Chong, G., 2008, The role of inherited tectono-sedimentary architecture in the development of the central Andean mountain belt: Insights from the Cordillera de Domeyko: Journal of Structural Geology, v. 30, p. 1520–1539, https://doi.org/10.1016/j.jsg.2008.08.005.

Ardill, J., Flint, S., Chong, G., and Wilke, H., 1998, Sequence stratigraphy of the Mesozoic Domeyko Basin, northern Chile: Journal of the Geological Society of London, v. 155, p. 71–88.

Armijo, R., Lacassin, R., Coudurier-Curveur, A., and Carrizo, D., 2015, Coupled tectonic evolution of Andean orogeny and global climate: Earth-Science Reviews, v. 143, p. 1–35, https://doi.org/10.1016/j.earscirev.2015.01.005.

Arriagada, C., Cobbold, P., and Roperch, P., 2006, Salar de Atacama basin: A record of compressional tectonics in the central Andes since the mid-Cretaceous: Tectonics, v. 25, TC1008, https://doi.org/10.1029/2004TC001770.

Arriagada, C., Roperch, P., Mpodozis, C., and Cobbold, P.R., 2008, Paleogene building of the Bolivian Orocline: Tectonic restoration of the central Andes in 2-D map view: Tectonics, v. 27, TC6014, https://doi.org/10.1029/2008TC002269.

Bascuñan, S., Arriagada, C., Le Roux, J., and Deckart, K., 2016, Unraveling the Peruvian phase of the Central Andes: Stratigraphy, sedimentology and geochronology of the Salar de Atacama Basin (22°30–23°S), northern Chile: Basin Research, v. 28, no. 3, p. 365–392, https://doi.org/10.1111/bre.12114.

Blanco, N., and Tomlinson, A., 2013, Carta Guatacondo, Región de Tarapacá: Servicio Nacional de Geología y Minería (Chile), Carta Geológica de Chile, N°156, scale 1:100,000, 116 p.

Blanco, N., Vásquez, P., Sepúlveda, F., Tomlinson, A., Quezada, A., and Ladino, M., 2012, Levantamiento geológico para el fomento de la exploración de recursos minerales e hídricos de la Cordillera de la Costa, Depresión Central y Precordillera de la Región de Tarapacá (20°–21°S): Servicio Nacional de Geología y Minería (Chile), 246 p.

Bonini, M., Sani, F., and Antonielli, B., 2012, Basin inversion and contractional reactivation of inherent normal faults: A review based on previous and new experimental model: Tectonophysics, v. 522, p. 55–88, https://doi.org/10.1016/j.tecto.2011.11.014.

Carrera, N., Muñoz, J.A., Sàbat, F., Roca, E., and Mon, R., 2006, The role of inversion tectonics in the structure of the cordillera oriental (NW Argentinean Andes): Journal of Structural Geology, v. 28, p. 1921–1932, https://doi.org/10.1016/j.jsg.2006.07.006.

Charrier, R., Pinto, L., and Rodríguez, M.P., 2007, Tectonostratigraphic evolution of the Andean Orogen in Chile, *in* Moreno, T., and Gibbons, W., eds., The Geology of Chile: Geological Society of London, p. 21–114.

Charrier, R., Farías, M., and Maksaev, V., 2009, Evolución tectónica, paleogeográfica y metalogénica durante el Cenozoico en los Andes de Chile Norte y Central e implicancias para las regiones adyacentes de Bolivia y Argentina: Revista de la Asociación Geológica Argentina, v. 65, p. 5–35.

Charrier, R., Hérail, G., Pinto, L., García, M., Riquelme, R., Farías, M., and Muñoz, N., 2013, Cenozoic tectonic evolution the Central Andes in northern Chile and west central Bolivia: Implications for paleogeographic, magmatic and mountain building evolution: International Journal of Earth Sciences, v. 102, p. 235–264, https://doi.org/10.1007/s00531-012-0801-4.

Coira, B., Davidson, J., Mpodozis, C., and Ramos, V.A., 1982, Tectonic and Magmatic Evolution of the Andes of Northern Argentina and Chile: Earth-Science Reviews, v. 18, p. 303–332, https://doi.org/10.1016/0012-8252(82)90042-3.

Cortés, J., Farías, M., Comte, D., and Charrier, R., 2012, Estructuras y depósitos neógenos de la región de Cariquima (Altiplano chileno): Implicancias en el origen de la Cordillera Occidental a los 19°30′S: Antofagasta, Congreso Geológico Chileno, no. 13, Actas, p. 229–231.

Farías, M., Charrier, R., Comte, D., Martinod, J., and Hérail, G., 2005, Late Cenozoic deformation and uplift of the western flank of the Altiplano: Evidence from the depositional, tectonic, and geomorphologic evolution and shallow seismic activity (northern Chile at 19°30′S): Tectonics, v. 24, TC4001, https://doi.org/10.1029/2004TC001667.

Flint, S., Turner, P., Jolley, E.J., and Hartley, A.J., 1993, Extensional tectonics in convergent margin basins: An example from the Salar de Atacama, Chilean Andes: Geological Society of America Bulletin, v. 105, p. 603–617, https://doi.org/10.1130/0016-7606(1993)105<0603:ETICMB>2.3.CO;2.

Franzese, J.R., and Spalletti, L.A., 2001, Late Triassic–early Jurassic continental extension in southwestern Gondwana: Tectonic segmentation and pre-break-up rifting: Journal of South American Earth Sciences, v. 14, p. 257–270, https://doi.org/10.1016/S0895-9811(01)00029-3.

Fuentes, G., Arriagada, C., and Martínez, F., 2016, Influencia de la estructura de la Cuenca de Tarapacá en el desarrollo del frente cordillerano occidental de los Andes Centrales: Evidencias en el borde oeste de la Cordillera de Domeyko (20°45′S): Santiago, Simposio de Tectónica Latinoamerica, no. 1, Actas, p. 54.

Fuentes, G., Martínez, F., and Arriagada, C., 2017, Estructura de la Cuenca de Tarapacá en la Pampa del Tamarugal, Norte de Chile (20°30′–21°S): Tucumán, Congreso Geológico Argentino, no. 20, Acta Simposio 12 Tectónica de los Andes argentino-chilenos, p. 104–109.

Gallardo, A., 1961, Informe geológico sobre el pozo de exploración Pintados-1, Provincia de Tarapacá: Empresa Nacional del Petróleo, Informe inédito, 72 p.

Gallardo, F., 2015, Geología y estructura de la Precordillera Altiplánica entre 19°45′ y 20°00′S, Región de Tarapacá, Chile [M.S. thesis]: Santiago, Universidad de Chile, 129 p.

Galli, C., and Dingman, I., 1962, Cuadrángulos Pica, Alca, Matilla y Chacarilla, con un estudio sobre los recursos de agua subterránea, Provincia de Tarapacá, Carta Geol. Chile, 3, 125 p.

Galli-Olivier, C., 1967, Pediplain in northern Chile and the Andean uplift: Science, v. 158, p. 653–655, https://doi.org/10.1126/science.158.3801.653.

García, M., and Hérail, G., 2005, Fault-related folding, drainage network evolution and valley incision during the Neogene in the Andean Precordillera of Northern Chile: Geomorphology, v. 65, p. 279–300, https://doi.org/10.1016/j.geomorph.2004.09.007.

Hardy, S., and Poblet, J., 1994, Geometric and numerical model of progressive limb rotation in detachment folds: Geology, v. 22, p. 371–374, https://doi.org/10.1130/0091-7613(1994)022<0371:GANMOP>2.3.CO;2.

Haschke, M., and Günther, A., 2003, Balancing crustal thickening in arcs by tectonic vs. magmatic means: Geology, v. 31, no. 11, p. 933–936, https://doi.org/10.1130/G19945.1.

Herrera, S., Pinto, L., Deckart, K., Cortés, J., and Valenzuela, J.I., 2017, Cenozoic tectonostratigraphic evolution and architecture of the Central Andes in northern Chile based on the Aquine region, Western Cordillera (19°–19°30′ S): Andean Geology, v. 44, p. 87–122, https://doi.org/10.5027/andgeoV44n2-a01.

Iaffa, D., Sàbat, F., Muñoz, F.A., Mon, R., and Gutierrez, A.A., 2011, The role of inherited structures in a foreland basin evolution. The Metán Basin in NW Argentina: Journal of Structural Geology, v. 33, p. 1816–1828, https://doi.org/10.1016/j.jsg.2011.09.005.
Isacks, B., 1988, Uplift of the Central Andean Plateau and Bending of the Bolivian Orocline: Journal of Geophysical Research, v. 93, p. 3211–3231, https://doi.org/10.1029/JB093iB04p03211.
Jordan, T.E., Mpodozis, C., Muñoz, N., Blanco, N., Pananont, P., and Gardeweg, M., 2007, Cenozoic subsurface stratigraphy and structure of the Salar de Atacama Basin, northern Chile: Journal of South American Earth Sciences, v. 23, p. 122–146, https://doi.org/10.1016/j.jsames.2006.09.024.
Jordan, T.E., Nester, P.L., Blanco, N., Hoke, G.D., Dávila, F., and Tomlinson, A.J., 2010, Uplift of the Altiplano-Puna plateau: A view from the west: Tectonics, v. 29, TC5007, https://doi.org/10.1029/2010TC002661.
Kley, J., and Monaldi, C.R., 2002, Tectonic inversion in the Santa Barbara System of the central Andean foreland thrust belt, northwestern Argentina: Tectonics, v. 21, p. 1061, https://doi.org/10.1029/2002TC902003.
Kley, J., Monaldi, C.R., and Salfity, J.A., 1999, Along-strike segmentation of the Andean foreland: Causes and consequences: Tectonophysics, v. 301, p. 75–94, https://doi.org/10.1016/S0040-1951(98)90223-2.
Labbé, N., García, M., Charrier, R., Araya, J., and Simicic, Y., 2015, Deformación sub-superficial en la cuenca Pampa del Tamarugal, Norte de Chile (22°30′S): La Serena, Congreso Geológico Chileno, no. 14, Actas, p. 225–229.
Legrand, D., Delouis, B., Dorbath, L., David, C., Campos, J., Marquéz, L., Thompson, J., and Comte, D., 2007, Source parameters of Mw=6.3 Aroma crustal earthquake of July 24, 2001 (northern Chile), and its aftershock: Journal of South American Earth Science, v. 24, p. 58–68.
López, C., Riquelme, R., Martínez, F., Sánchez, C. and Mestre, A., 2017, Zircon U-Pb geochronology of the Mesozoic to lower Cenozoic rocks of the Coastal Cordillera in the Antofagasta region (22°30′–23°00′S): Insights to the Andean tectono-magmatic evolution: Journal of South American Earth Sciences, 26 p., https://doi.org/10.1016/j.jsames.2017.11.005 (in press).
Lowell, J.D., 1995, Mechanisms of basin inversion from worldwide examples, *in* Buchanan, J.P., and Buchanan, P.G., eds., Basin Inversion: Geological Society of London Special Publication 88, p. 39–57, https://doi.org/10.1144/GSL.SP.1995.088.01.04.
Maksaev, V., and Zentilli, M., 1999, Fission Track Thermochronology of the Domeyko Cordillera, Northern Chile: Implications for Andean Tectonics and Porphyry Copper Metallogenesis: Exploration and Mining Geology, v. 8, p. 65–89.
Martínez, F., Arriagada, C., Peña, M., Del Real, I., and Deckart, K., 2013, The structure of the Chañarcillo Basin: An example of tectonic inversion in the Atacama region, northern Chile: Journal of South American Earth Sciences, v. 42, 16 p., https://doi.org/10.1016/j.jsames.2012.07.001.
Martínez, F., Arriagada, C., Peña, M., Deckart, K., and Charrier, R., 2016, Tectonic styles and crustal shortening of the Central Andes "Pampean" flat-slab segment in northern Chile (27°–29°S): Tectonophysics, v. 667, p. 144–162, https://doi.org/10.1016/j.tecto.2015.11.019.
Martínez, F., González, R., Bascuñan, S., and Arriagada, C., 2017, Structural styles of the Salar de Punta Negra Basin in the Preandean Depression (24°–25°S) of the Central Andes: Journal of South American Earth Sciences, https://doi.org/10.1016/j.jsames.2017.08.004 (in press).
Mégard, F., 1984, The Andean orogenic period and its major structures in central and northern Peru: Journal of the Geological Society of London, v. 141, p. 893–900, https://doi.org/10.1144/gsjgs.141.5.0893.
Mitchum, R.M., Jr., Vail, P.R., and Thompson, S., III, 1977, Seismic stratigraphy and global changes of sea level; Part 2, The depositional sequence as a basic unit for stratigraphic analysis, *in* Payton, C.E, eds., Seismic Stratigraphy: Applications to Hydrocarbon Exploration: American Association of Petroleum Geologists Memoir, v. 26, p. 53–62.
Mitra, S., 1993, Geometry and kinematic evolution of inversion structures: American Association of Petroleum Geologists Bulletin, v. 77, p. 1159–1191.
Mordojovich, C., 1965, Reseña sobre las exploraciones de la ENAP en la zona norte, años 1956 a 1962: Minerales, v. 20, p. 32–61.
Mortimer, C., 1973, The Cenozoic history of the southern Atacama desert, Chile: Journal of the Geological Society of London, v. 129, p. 505–526, https://doi.org/10.1144/gsjgs.129.5.0505.
Mpodozis, C., and Ramos, V.A., 1989, The Andes of Chile and Argentina, *in* Ericksen, G.E., Cañas Pinochet, M.T., and Reinemund, J.A., eds., Geology of the Andes and Its Relation to Hydrocarbon and Mineral Resources: Houston, Texas, Circum-Pacific Council for Energy and Mineral Resources Earth Sciences Series, v. 11, p. 59–90.
Mpodozis, C., and Ramos, V.A., 2008, Tectónica jurásica en Argentina y Chile: Extensión, subducción oblicua, rifting, deriva y colisiones?: Revista de la Asociación Geológica Argentina, v. 63, p. 481–497.
Mpodozis, C., Arriagada, C., Basso, M., Roperch, P., Cobbold, P., and Reich, M., 2005, Late Mesozoic to Paleogene stratigraphy of the Salar de Atacama basin, Antofagasta, northern Chile: Implications for the tectonic evolution of the central Andes: Tectonophysics, v. 399, p. 125–154, https://doi.org/10.1016/j.tecto.2004.12.019.
Muñoz, N., and Charrier, R., 1996, Uplift of the western border of the Altiplano on a west-vergent thrust system, Northern Chile: Journal of South American Earth Sciences, v. 9, p. 171–181, https://doi.org/10.1016/0895-9811(96)00004-1.
Muñoz, N., and Sepúlveda, P., 1992, Estructuras compresivas con vergencia al oeste en el borde oriental de la Depresión Central, Norte de Chile (19°15′S): Revista Geológica de Chile, v. 19, p. 241–247, 10.5027/andgeoV19n2-a07.
Nester, P., 2008, Basin and paleoclimate evolution of the Pampa del Tamarugal forearc valley, Atacama Desert, Northern Chile [Ph.D. thesis]: Ithaca, Cornell University, 256 p.
Nester, P.L., and Jordan, T.E., 2012, The Pampa del Tamarugal forearc basin in Northern Chile: The interaction of tectonics and climate, *in* Busby, C., and Azor, A., eds., Tectonics of Sedimentary Basins: Recent Advances: Oxford, England, Blackwell Publishing Ltd., p. 369–381, https://doi.org/10.1002/9781444347166.ch18.
Pananont, P., Mpodozis, C., Blanco, N., Jordan, T.E., and Brown, L.D., 2004, Cenozoic evolution of the northwestern Salar de Atacama Basin, northern Chile: Tectonics, v. 23, TC6007, https://doi,org/10.1029/2003TC001595.
Pardo-Casas, F., and Molnar, P., 1987, Relative motion of the Nazca (Farallon) and South American plates since Late Cretaceous time: Tectonics, v. 6, no. 3, p. 233–248, https://doi.org/10.1029/TC006i003p00233.
Pinto, L., Hérail, G., and Charrier, R., 2004, Sedimentación sintectónica asociada a las estructuras neógenas en la Precordillera de la zona de Moquella, Tarapacá (19°15′S, norte de Chile): Revista Geológica de Chile, v. 31, p. 19–44, https://doi.org/10.4067/S0716-02082004000100002.
Ramos, V.A., 2010, The tectonic regime along the Andes: Present-day and Mesozoic regimes: Geological Journal, v. 45, no. 1, p. 2–25, https://doi.org/10.1002/gj.1193.
Sepúlveda, F., Vásquez, P., and Quezada, A., 2012, Carta Patillos y Oficina Victoria, Región de Tarapacá: Servicio Nacional de Geología y Minería (Chile), Carta Geológica de Chile, N°167–168, scale 1:100,000, 107 p.
Somoza, R., 1998, Updated Nazca (Farallón)–South America relative motions during the last 40 My: Implications for mountain building in the central Andean region: Journal of South American Earth Sciences, v. 11, no. 13, p. 211–215, https://doi.org/10.1016/S0895-9811(98)00012-1.
Steinmann, G., 1929, Geologie von Peru: Heidelberg, Kart Winter, 448 p.
Tobar, A., Salas, R., and Kast, R., 1968, Carta Geológica de Chile, Cuadrángulos Camaraca y Azapa, Provincia de Tarapacá: Instituto de Investigaciones Geológicas, Carta Geológica de Chile, v. 19–20, 25 p.
Tomlinson, A., Blanco, N., Maksaev, V., Dilles, J.H., Grunder, A.L., and Ladino, M., 2001, Geología de la Precordillera Andina de Quebrada Blanca-Chuquicamata, Regiones I y II (20°30′–22°30′S): Santiago, Servicio Nacional de Geología y Minería, Infome Registrado IR-01-20, 444 p.
Vail, P.R., Mitchum, R.M., Jr., and Thompson, S., III, 1977, Seismic stratigraphy and global changes of sea level; Part 4, Global cycles of relative changes of sea level, *in* Payton, C.E., ed., Seismic Stratigraphy; Applications to Hydrocarbon Exploration: American Association of Petroleum Geologists Memoir 26, p. 83–97.
Vergés, J., Fernández, M., and Martínez, A., 2002, The Pyrenean orogen: Pre-, syn-, and post-collisional evolution, *in* Rosenbaum, G., and Lister, G.S., eds., Reconstruction of the Evolution of the Alpine-Himalayan Orogen: Journal of the Virtual Explorer, v. 8, p. 55–74, https://doi.org/10.3809/jvirtex.2002.00058.
Vicente, J.C., 2006, Dynamic Paleogeography of the Jurassic Andean Basin: Pattern of regression and general considerations on main features: Revista de la Asociación Geológica Argentina, v. 61, p. 408–437.
Victor, P., Oncken, O., and Glodny, J., 2004, Uplift of the western Altiplano plateau: Evidence from the Precordillera between 20° and 21°S (northern Chile): Tectonics, v. 23, TC4004, https://doi.org/10.1029/2003TC001519.
Yamada, Y., and McClay, K., 2004, 3-D Analog modeling of inversion thrust structures, *in* McClay, K., ed., Thrust Tectonics and Hydrocarbon Systems: American Association of Petroleum Geologists Memoir 82, p. 276–301.